Acta Crystallographica Section D
Biological Crystallography
ISSN 0907-4449

Structure of human erythrocyte NADH-cytochrome b_5 reductase

Sachiko Bando,[a] Tsunehiro Takano,[a]* Toshitsugu Yubisui,[b,c] Komei Shirabe,[b] Masazumi Takeshita[b] and Atsushi Nakagawa[a]

[a]Institute for Protein Research, Osaka University, 3-2 Yamadaoka, Suita, Osaka 565-0871, Japan, [b]Oita University, Faculty of Medicine, Hazama-cho, Oita 879-5593, Japan, and [c]Okayama University of Science, Department of Biochemistry, Faculty of Science, 1-1 Ridai-cho, Okayama 700-0005, Japan

Correspondence e-mail: ttakano@protein.osaka-u.ac.jp

Received 27 April 2004
Accepted 20 August 2004

PDB References: NADH-cytochrome b_5 reductase, 1umk, r1umksf

Erythrocyte NADH-cytochrome b_5 reductase reduces methaemoglobin to functional haemoglobin. In order to examine the function of the enzyme, the structure of NADH-cytochrome b_5 reductase from human erythrocytes has been determined and refined by X-ray crystallography. At 1.75 Å resolution, the root-mean-square deviations (r.m.s.d.) from standard bond lengths and angles are 0.006 Å and 1.03°, respectively. The molecular structure was compared with those of rat NADH-cytochrome b_5 reductase and corn nitrate reductase. The human reductase resembles the rat reductase in overall structure as well as in many side chains. Nevertheless, there is a large main-chain shift from the human reductase to the rat reductase or the corn reductase caused by a single-residue replacement from proline to threonine. A model of the complex between cytochrome b_5 and the human reductase has been built and compared with that of the haem-containing domain of the nitrate reductase molecule. The interaction between cytochrome b_5 and the human reductase differs from that of the nitrate reductase because of differences in the amino-acid sequences. The structures around 15 mutation sites of the human reductase have been examined for the influence of residue substitutions using the program *ROTAMER*. Five mutations in the FAD-binding domain seem to be related to cytochrome b_5.

1. Introduction

NADH-cytochrome b_5 reductase (b5R; EC 1.6.2.2), an enzyme containing FAD (flavin adenine dinucleotide; Strittmatter, 1965; Iyanagi *et al.*, 1984), is known to exist in both membrane-bound and soluble forms. The membrane-bound form, which is embedded mainly in the endoplasmic reticulum membrane as an amphipathic protein, participates in a variety of metabolic transformations, such as desaturation and elongation of fatty acids (Oshino *et al.*, 1971; Keyes & Cinti, 1980), cholesterol biosynthesis (Reddy *et al.*, 1977) and cytochrome P450-dependent drug metabolism (Hildebrant & Estabrook, 1971). The soluble form in erythrocytes is involved in the electron-transport system for reducing methaemoglobin to functional haemoglobin (Hultquist & Passon, 1971). The soluble enzyme is formed by an alternative splicing of the erythroid exon and by liver axons 2–9, but the erythroid exon does not make a 'sense' peptide. Therefore, the origin of residues 26–300 of the soluble enzyme is the same as the membrane-bound form of the enzyme (Du *et al.*, 1997).

Deficiency of b5R causes two types of hereditary methaemoglobinaemia: an erythrocyte type (type I; Scott & Griffith, 1959) and a generalized type (type II; Leroux *et al.*, 1975). The former arises from enzyme deficiency in erythro-

cytes and causes mild cyanosis. The latter arises from generalized deficiency of the enzyme in all tissues and causes physical and mental growth retardation and other neurological defects.

Human erythrocyte b5R is a member of the ferredoxin-$NADP^+$ reductase (FNR; Karplus *et al.*, 1991; Bruns & Karplus, 1995) superfamily. This family includes phthalate dioxygenase reductase (PDR; Correll *et al.*, 1992, 1993), corn nitrate reductase (RNR; Lu *et al.*, 1994, 1995) and liver microsomal NADH-cytochrome b_5 reductase from pig (Nishida, Inaka & Miki, 1995; Nishida, Inaka, Yamanaka *et al.*, 1995) and rat (Bewley *et al.*, 2001), the three-dimensional structures of which have been determined by X-ray crystallography. The overall molecular structure of human b5R determined by the previous structure analysis at 2.5 Å resolution can be seen to be essentially the same as other enzymes in the family (Takano *et al.*, 1994).

Here, we report the crystal structure of human erythrocyte b5R at 1.75 Å resolution and compare the structure of the enzyme with those of rat b5R (PDB codes 1i7p and 1ib0) and RNR (PDB code 2cnd).

2. Materials and methods

The human erythrocyte b5R used in this study was expressed in *Escherichia coli* as described previously (Shirabe *et al.*, 1989). The soluble form of the enzyme was overexpressed as an α-thrombin-cleavable fusion protein.

2.1. Crystallization

Crystals of the human b5R were grown by the sitting-drop vapour-diffusion method as described previously (Takano *et al.*, 1987); that is, 30%(*w*/*v*) PEG 4000 solution pH 7.6 was gradually added to a drop of 20 µl 6%(*w*/*v*) protein solution pH 7.6 under a microscope until amorphous precipitate remained insoluble for a few minutes. Crystals grew within the amorphous precipitate in the 20 µl droplet of about 6%(*w*/*v*) PEG concentration. Growing crystals in the sitting drop were left at room temperature until the amorphous precipitate completely dissolved and then kept at 286 K until they reached full size. Crystals were transferred to synthetic mother liquor containing 25%(*w*/*v*) PEG 4000 with 17% glycerol as cryoprotectant before X-ray data collection.

2.2. X-ray data collection

X-ray diffraction intensities were measured to 1.7 Å resolution at 100 K in a liquid-nitrogen gas stream using a Rigaku R-AXIS IV imaging-plate detector mounted on a Rigaku Ultra X18 rotating-anode generator operated at 40 kV, 100 mA and equipped with an Osmic Multilayer Optical mirror system. The crystal-to-detector distance was 120 mm. A total of 130 frames were collected with an interval of 1.0° and 20 min exposure per frame. The intensity data collected from a single crystal were scaled and merged using *MOSFLM*, *SCALA* and *TRUNCATE* from the *CCP*4 program suite (Collaborative Computational Project, Number 4, 1994). The overall temperature factor B evaluated by a Wilson plot was 28.0 $Å^2$.

Table 1
Crystallographic data and refinement statistics.

Crystallographic data	
Space group	$P4_1$
Unit-cell parameters	
$a = b$ (Å)	65.87
c (Å)	76.20
Resolution range† (Å)	35.00–1.75 (23.70–1.75)
No. measured reflections	286342
No. unique reflections†	32692 (32639)
No. >3σ	29304
Completeness‡ (%)	99.4 (98.1)
R_{sym}‡	0.05 (0.128)
$I/\sigma(I)$‡	8.7 (5.4)
Multiplicity‡	5.2 (4.7)
Refinement	
No. working reflections‡	30988 (2261)
No. free reflections‡	1651 (115)
R_{work}‡	0.165 (0.24)
R_{free}‡	0.208 (0.25)
R.m.s.d., bond lengths (Å)	0.006
R.m.s.d., bond angles (°)	1.03
No. protein atoms§	2226
No. water molecules	753
Average B value for all atoms ($Å^2$)	24.1
Average B value for main chain	17.0
Average B value for side chain and waters	28.2
Average r.m.s. B for 271 main-chain residues	0.377
Average r.m.s. B for 241 side-chain residues	0.995

† Value in parentheses is that used for refinement. ‡ Value in parentheses is for the highest resolution shell. § Value includes eight alternate atoms.

2.3. Structure refinement

The structure of the enzyme was previously determined at 2.5 Å resolution (unpublished work) using the MIRAS method with the intensity data from a native crystal and three heavy-atom derivatives collected at 286 K and refined to a crystallographic R factor of 21%. The crystal belongs to the tetragonal space group $P4_1$, with unit-cell parameters $a = b = 65.87$, $c = 76.20$ Å. The handedness of the intensity data was determined by comparison with the 2.5 Å resolution data.

The present structure analysis at 1.75 Å resolution started with the atomic coordinates of the 2.5 Å structure as an initial model. After rotational and translational parameters for the present crystal had been determined using the program *MOLREP*, the electron-density map was improved by the programs *SFALL*, *SIGMAA*, *DM* and *FFT*. The model was manipulated using the program *O* (Jones *et al.*, 1991) and refined with the program *REFMAC*5. The restrained maximum-likelihood method was employed. The program *ARP*/*wARP* automatically picked up solvent molecules during the refinement cycles. The final model consists of 2971 non-H atoms, including 2218 protein atoms and 753 water molecules. Analysis of the stereochemical quality of the structure using *PROCHECK* (Laskowski *et al.*, 1993) is excellent and 93% of the non-glycine and non-proline residues are in most favoured regions; the remaining 16 residues are in additional allowed regions. The overall G factor is 0.15. The average coordinate

error evaluated by a Luzzati plot (Luzzati, 1952) is 0.17 Å. Statistics of the structure refinement are listed in Table 1.[1]

3. Results and discussion

Although the α-thrombin-cleaved enzyme was determined to have an amino-acid sequence consisting of residues 26–300, the electron-density map of the current study revealed the first residue to be Thr30; *i.e.* the first four residues (Phe26-Gln27-Arg28-Ser29) were invisible in electron-density maps.

3.1. Features of three-dimensional structure

The molecular structure of b5R (Fig. 1) consists of two major domains: the N-terminal or FAD-binding domain (Thr30–Ser145) and the C-terminal or NADH-binding domain (Ser173–Phe300). These two domains are connected by a small linker domain (Gly146–Lys172) consisting of a triple-stranded antiparallel β-sheet (Lβ1–Lβ3) (Fig. 2). A cofactor FAD is non-covalently bound in a large and wide boundary cleft between the two major domains.

The FAD-binding domain consists of three prominent structural features: a six-stranded antiparallel β-barrel (Fβ1–Fβ6) with a Greek-key motif, an α-helix Fα1 (Gly124–Met133) and a long loop (Val111–Gly123). The arrangement of the α-helices and the β-strands in the NADH-binding domain is to form three β1–α–β2 motifs: Nβ1–Nα1–Nβ2 (Ser173–Asn209), Nβ2–Nα3–Nβ3 (Val202–Leu238) and Nβ5–Nα6–Nβ6 (Leu269–Phe300). The first motif is typical of the NAD$^+$-binding motif (Rossmann *et al.*, 1974, 1975), in which the glycine-rich loop (Gly179–Gly182) forms a 3_{10}-turn and is in close contact with the ADP part of NAD$^+$ in rat b5R (Bewley *et al.*, 2001).

Tyr247 has unusual main-chain torsion angles, (φ, ψ) = (−122.5, −151.0) and is barely in the allowed region of the Ramachandran plot. The residue makes no special contacts with surrounding residues, except for a hydrogen bond between the Tyr247 OH atom and a water molecule (2.78 Å). Similar values were also found for the corresponding tyrosine residues: (φ, ψ) = (−108.4, −154.1) for rat b5R, (−106.9, −165.8) for RNR and (−107.6, −137.6) for pig b5R.

The α-helix Fα1 is oriented to allow its α-helical dipole to stabilize the negative charges of the diphosphate group of the FAD (Karplus *et al.*, 1991; Wierenga *et al.*, 1985). In addition to the interaction, another α-helix seems to interact with negative charges in the NADH-binding domain. α-Helix Nα1 (Gly182–Lys195) is followed by three aspartic acid residues: Asp196, Asp198 and Asp199. The aspartic negative charges located at the C-terminal end of the α-helix should reinforce the helix dipole moment and the

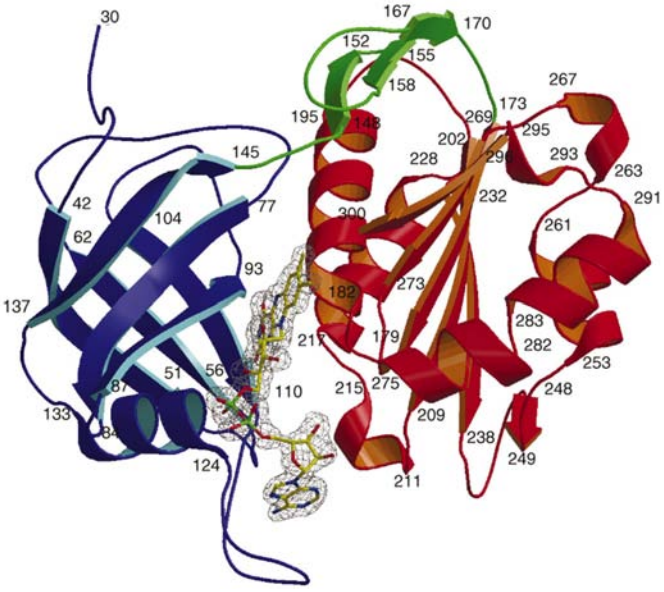

Figure 1
Overview of the human b5R structure with residue numbers at the beginning and the end of the secondary structures. A ball-and-stick model of FAD is superposed on an 'omit' electron-density map contoured at 0.8σ. The FAD-binding domain is in blue, the NADH-binding domain in red and the linker domain in green. This figure was drawn using *MOLSCRIPT* (Kraulis, 1991), *BOBSCRIPT* (Esnouf, 1997) and *RASTER3D* (Merritt & Bacon, 1997).

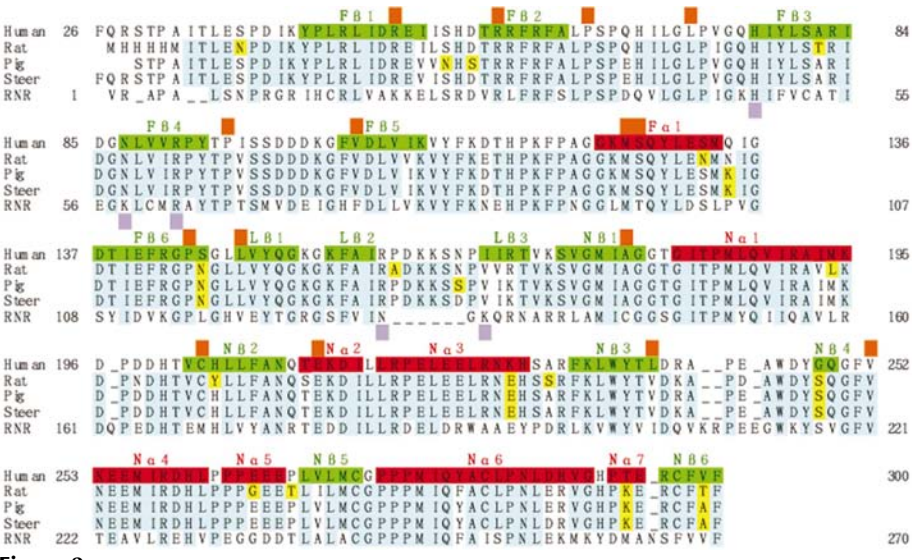

Figure 2
Sequence alignment of human, rat, pig and steer b5R (Strittmatter *et al.*, 1992) and RNR. The RNR sequence is aligned based on the three-dimensional structures. The background colours indicate the secondary structures of human b5R: green for β-strand, red for α-helix and white for loop. Cyan represents residues that are identical to human b5R and yellow represents residues that are non-homologous to human b5R. Orange rectangles indicate mutation sites of human b5R and magenta rectangles below RNR indicate residues that interact with cytochrome b_5 (Lu *et al.*, 1995).

[1] Supplementary material has been deposited in the IUCr electronic archive (Reference: AD5018). Services for accessing these data are described at the back of the journal.

stronger dipole should be advantageous for the stabilization of negative charges on NADH at the N-terminal end of the helix. In fact, the nicotinamide-ribose O atoms of NAD^+ in rat b5R are close to the N-terminal end of the helix and the following diphosphate group of NAD^+ closely interacts with the glycine-rich region (Gly179–Gly182) at the beginning of the α-helix (Bewley *et al.*, 2001).

Four residues, Thr56, Val90, Val108 and Ser145, apparently have alternate side-chain conformations. Rotation around the CA–CB bond of the valine residues places one of the CG atoms at the other CG atom position to make the latter CG-atom position common to an alternate form of the side chain. The electron density for the Ser145 side chain has three peaks for the OG atom: one of the alternate OG atom positions forms a hydrogen bond to the NE2 atom of His77 (2.64 Å), while the other two OG atom positions point toward the solvent.

The amino-acid sequence is well conserved among the mammalian species, as shown in Fig. 2. 38 residues in the human b5R sequence (Ile33–Phe300) are different from the other three mammalian b5R sequences, in which 18 changes are non-homologous: eight at residues 37, 53, 55, 134, 160, 165, 230 and 268 in loop regions, and ten at residues 82, 132, 145, 194, 204, 227, 248, 265, 294 and 299 in the α-helical and β-strand regions. The small number of non-homologous changes in the loop regions seems to suggest that the loop structures are stable and functional. The long loop from Val111 to Gly123, whose residues are invariant except for the homologous Asp115, is indeed important to stabilize the adenine moiety of FAD by a hydrogen bond between the amino N atom AN6 of the adenine ring and the Phe113 O atom (2.79 Å). Unlike corn nitrate reductase (RNR; Lu *et al.*, 1994, 1995), the parallelism between the adenine ring and the aromatic rings of the loop is no longer retained in human b5R (the angle between the two planes being 63° for Tyr112 and 48° for His117), except for Phe120 where the angle between them is 6.7°.

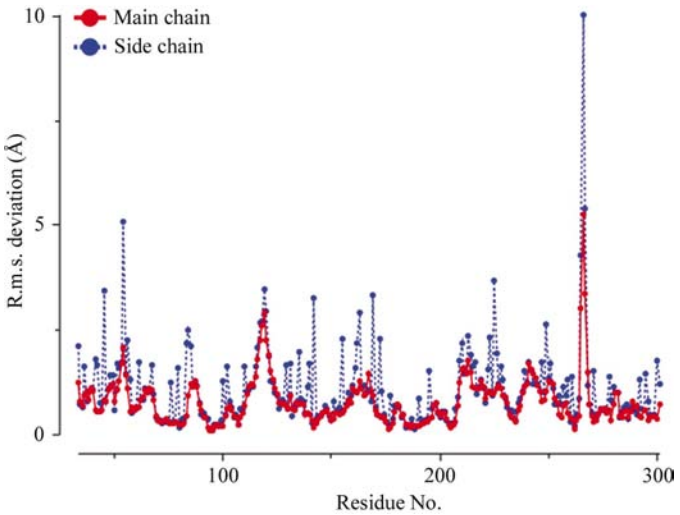

Figure 3
The root-mean-square deviation in Å between common atoms of human b5R and rat b5R *versus* residue numbers. The deviation for the main-chain atoms is indicated in red and that for the side-chain atoms in blue. This figure was produced using *LOGGRAPH* from the *CCP*4 program suite.

The program *ARP*/*wARP* automatically counted a total of 753 water molecules in the refinement cycles with *REFMAC*5. 30 water molecules of the 39 that were located within the molecular surface are common to both human and rat b5R. Two water molecules of the 15 bound to FAD are internally located and also bound to protein atoms. The first water molecule is hydrogen bonded to the isoalloxazine O2 atom (2.65 Å), the ribityl O4* atom (2.72 Å) and the Lys110 O atom (2.65 Å). The second water molecule is bonded to the isoalloxazine O4 atom (2.83 Å), the Thr94 O atom (2.69 Å) and the Val108 N atom (2.68 Å). These two water molecules were also found in rat b5R (Bewley *et al.*, 2001), RNR (Lu *et al.*, 1995), FNR (Correll *et al.*, 1993) and PDR (Correll *et al.*, 1992).

3.2. Comparison with Rat b5R

The relative positions of the two major domains of human b5R resemble those of rat b5R when the main chains are compared. The rotation required to superpose (Kabsch, 1976) the two domains is only 3.0°. Similarly, the rotation required to superpose the linker domains is 2.1°.

Although the overall structure is remarkably conserved in both human and rat b5R, there is a large main-chain shift in the region of residues Glu265–Pro268, which has amino-acid sequence EEEP in human b5R (Fig. 3). The different conformation of the region is stabilized by a hydrogen-bonding system in each molecule: Glu267 O···Arg169 NH2, Glu267 N···Pro264 O and Glu267 OE2···Arg296 NH2 in human b5R, and Glu267 O···Ser173 N and Glu267 OE2···Lys172 NZ in rat b5R. The cause of the conformational change in this region can be attributed to the substitution Pro268Thr, as pig b5R (PDB code 1ndh; Nishida, Inaka & Miki, 1995) has the same sequence as human b5R (Yubisui *et al.*, 1984) and has the same conformation in this region. On the other hand, RNR, which has the amino-acid sequence GDDT in this region (Hyde *et al.*, 1991), has the same conformation as rat b5R, whose sequence is GEET.

The largest deviation for all atoms is found at Glu266 OE2 (14.3 Å) when residues 265–268 are included and is found at His54 NE2 (7.6 Å) when residues 265–268 are excluded (His54, which is located in the loop between Fβ1 and Fβ2, has a torsion angle around the CA—CB bond $\chi_1 = +69°$ in human b5R and $\chi_1 = -179°$ in rat b5R, so that the His54 imidazole rings are in very different positions). For the main-chain atoms, the largest deviation is 5.7 Å at Glu266 CA when residues 265–268 are included and is 3.0 Å at Lys119 CA when residues 265–268 are excluded. The residues His54, Lys119 and Glu266 are well defined in the electron-density map.

3.3. Similarity to RNR

The amino-acid sequence of RNR (Hyde *et al.*, 1991) was aligned with human b5R (Fig. 2) by comparing only CA-atom positions because of the large difference in amino-acid composition. RNR only has 43% identity with human b5R,

whereas rat b5R has 86% identity with human b5R. Nevertheless, the overall three-dimensional structures of human b5R and RNR very much resemble each other; the root-mean-square deviation of CA atoms in the secondary structures of the two protein molecules is only 0.9 Å and the rotation angle needed to superpose the two major domains is only 0.4°. The 15 residues of RNR where mutations occur in human b5R (Fig. 2) are homologous with regard to polarity.

3.4. Model of b5–b5R complex

The model for the haem-containing domain of nitrate reductase (NR; Lu *et al.*, 1995) based on bovine b5 and RNR, namely the b5–RNR complex, was built on the condition that the haem and the isoalloxazine were as closely located as in flavocytochrome b_2 (Xia & Mathews, 1990). Five residues of RNR are involved in the interaction with the b5 molecule, including those between His48 of RNR and the haem propionate of b5, between Lys58 and Arg62 of RNR and Asp64 of b5, and between Asn130 and Lys132 of RNR and Asp44 of b5.

In a trial model for b5–b5R complex molecule between bovine b5 and human b5R with the same orientation of the haem plane and the isoalloxazine ring as in flavocytochrome b_2, the b5 molecule collides with the loops from residues 63 to 76 and from residues 94 to 103 in the FAD domain of b5R. The most probable model without collision between b5 and b5R turned out to be the same as the b5–RNR model. In this model, His77 is hydrogen bonded to the b5 propionate and the loops of the linkage domain of b5R are in contact with the side of the haem group, *i.e.* the invariant Gly146 is in close proximity to His77 and the carboxy group of the propionate, the invariant Leu147 is close to the propionate and the methyl group and the invariant Asp161 is close to the exposed vinyl group.

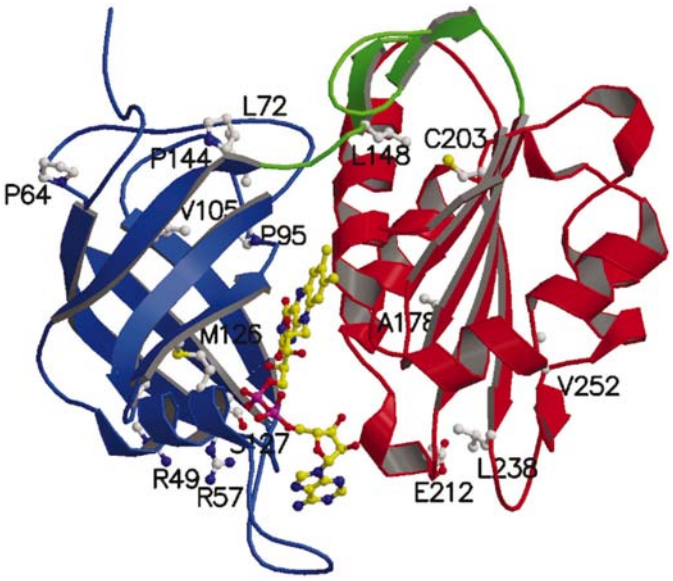

Figure 4
Locations of 15 mutation sites on human b5R. This figure was drawn using *MOLSCRIPT* and *RASTER3D*.

According to the sequence alignment (Fig. 2), some residues of RNR that contact b5 in the b5–RNR model are not homologous to those in human b5R: Lys58 in RNR corresponds to Asn87 in human b5R and similarly Asn130 corresponds to Arg159 and Lys132 corresponds to Ile167. These changes reduce the number of the interactions in b5–b5R, unless there are further amino-acid changes. There are, however, three more sites in b5R for new interactions with b5: interactions between the invariant Arg142 of b5R and Glu59 of b5 and similarly between the invariant Lys162 and Asp60 and between the invariant Lys163 and Glu56. These interactions seem to make b5–b5R as stable as b5–RNR with regard to the number of interactions.

The region of residues 265–268 with the large main-chain shift from rat b5R seems to have no biological function as it makes no interaction with b5.

3.5. Structural implication of mutation sites

We have examined the structural implication of the mutations for 15 mutation sites (Fig. 2) by replacing wild-type residues with mutant ones using the programs *O* and *ROTAMER* on a fixed main-chain atoms basis. The locations of the mutation sites are depicted in Fig. 4. Assuming the complex model to be correct, the effect of the mutations has been interpreted: the mutations in the FAD-binding domain seem to be related to either FAD binding or b5 binding, while all the mutations in the NAD^+-binding domain are related solely to the NAD^+ binding. The following five substitutions seem to perturb either His77 or the b5 propionate to make b5–b5R unstable.

(i) Pro64Leu (Dekker *et al.*, 2001). Pro64 in the long loop (Leu63–Gln76) is on the exposed molecular surface, making a tight turn at Pro64 that is kept stable by hydrogen bonds formed by Ser65, Gln67 and His68. The substitution causes a drastic conformational change and alters the main-chain path of the loop. The change should be propagated to His77.

(ii) Leu72Pro (Wu *et al.*, 1998). Leu72 is enclosed in a pocket formed by Val35, Leu70, Pro73, His77, Ile78, Pro95 and Pro144. The substitution should cause a large change of the main-chain path and perturb the proximal His77.

(iii) Val105Met (Shirabe *et al.*, 1992). Val105 is in van der Waals contact with Leu63, Leu70, Pro95 and Phe141. The larger side chain of Met105 should perturb Phe141 and the following sequence as far as Leu148, which is in contact with the b5 propionate.

(iv) Pro144Leu (Dekker *et al.*, 2001) and Leu148Pro (Nagai *et al.*, 1993; Katsube *et al.*, 1991). Both these substitutions alter the main-chain path because of the involvement of the proline residue. The sequence from Pro144 to Leu148 is in close contact with the b5 propionate and the substitutions should hinder the hydrogen bond between His77 and the propionate.

The authors express their thanks to Professor Tomitake Tsukihara for his kind support of the present work. We also thank to Miss Chihiro Horii for her eager work in enzyme

preparation and Mr Ken-ichi Sakaguchi for his kind help with X-ray intensity data collection.

References

Bewley, M. C., Marohnic, C. C. & Barber, M. J. (2001). *Biochemistry*, **40**, 13574–13580.

Bruns, C. M. & Karplus, P. A. (1995). *J. Mol. Biol.* **247**, 125–145.

Collaborative Computational Project, Number 4 (1994). *Acta Cryst.* D**50**, 760–763.

Correll, C. C., Batie, C. J., Ballou, D. P. & Ludwig, M. L. (1992). *Science*, **258**, 1604–1610.

Correll, C. C., Ludwig, M. L., Bruns, C. M. & Karplus, P. A. (1993). *Protein Sci.* **2**, 2112–2133.

Dekker, J., Eppink, M. H. M., van Zwieten, R., de Rijk, T., Remacha, A. F., Law, L. K., Li, A. M., Cheung, K. L., van Berkel, W. J. H. & Roos, D. (2001). *Blood*, **97**, 1106–1114.

Du, M., Shirabe, K. & Takeshita, M. (1997). *Biochem. Biophys. Res. Commun.* **235**, 779–783.

Esnouf, R. M. (1997). *J. Mol. Graph.* **15**, 132–134.

Hildebrant, A. & Estabrook, R. W. (1971). *Arch. Biochem. Biophys.* **143**, 66–79.

Hultquist, D. E. & Passon, P. G. (1971). *Nature New Biol.* **299**, 252–254.

Hyde, G. E., Crawford, N. M. & Campbell, W. H. (1991). *J. Biol. Chem.* **266**, 23542–23547.

Iyanagi, T., Watanabe, S. & Anan, K. F. (1984). *Biochemistry*, **23**, 1418–1425.

Jones, T. A., Cowan, S., Zou, J.-Y. & Kjeldgaard, M. (1991). *Acta Cryst.* A**47**, 110–119.

Kabsch, W. (1976). *Acta Cryst.* A**32**, 922–923.

Karplus, P. A., Daniels, M. J. & Herriott, J. R. (1991). *Science*, **251**, 60–66.

Katsube, T., Sakamoto, N., Kobayashi, Y., Seki, R., Hirano, M., Tanishima, K., Tomoda, A., Takazakura, E., Yubisui, T., Takeshita, M., Sakaki, Y. & Fukumaki, Y. (1991). *Am. J. Hum. Genet.* **48**, 799–808.

Keyes, S. R. & Cinti, D. L. (1980). *J. Biol. Chem.* **255**, 11357–11364.

Kraulis, P. J. (1991). *J. Appl. Cryst.* **24**, 946–950.

Laskowski, R. A., MacArthur, M. W., Moss, D. S. & Thornton, J. M. (1993). *J. Appl. Cryst.* **26**, 283–291.

Leroux, A., Junien, C., Kaplan, J.-C. & Bamberger, J. (1975). *Nature (London)*, **258**, 619–620.

Lu, G., Campbell, W. H., Schneider, G. & Lindqvist, Y. (1994). *Structure*, **2**, 809–821.

Lu, G., Lindqvist, Y., Schneider, G., Dwivedi, U. & Campbell, W. H. (1995). *J. Mol. Biol.* **248**, 931–948.

Luzzati, V. (1952). *Acta Cryst.* **5**, 802–810.

Merritt, E. A. & Bacon, D. J. (1997). *Methods Enzymol.* **276**, 505–524.

Nagai, T., Shirabe, K., Yubisui, T. & Takeshita, M. (1993). *Blood*, **81**, 808–814.

Nishida, H., Inaka, K. & Miki, K. (1995). *FEBS Lett.* **361**, 97–100.

Nishida, H., Inaka, K., Yamanaka, M., Kaida, S., Kobayashi, K. & Miki, K. (1995). *Biochemistry*, **34**, 2763–2767.

Oshino, N., Imai, Y. & Sato, R. (1971). *J. Biochem.* **69**, 155–167.

Reddy, V. V. R., Kupfer, D. & Capsi, E. (1977). *J. Biol. Chem.* **252**, 2797–2801.

Rossmann, M. G., Liljas, A., Branden, C.-I. & Banaszak, L. J. (1975). *Enzymes*, **11**, 61–102.

Rossmann, M. G., Moras, D. & Olsen, K. W. (1974). *Nature (London)*, **250**, 194–199.

Scott, E. M. & Griffith, I. V. (1959). *Biochim. Biophys. Acta*, **34**, 584–586.

Shirabe, K., Yubisui, T., Borgese, N., Tang, C. Y., Hultquist, D. E. & Takeshita, M. (1992). *J. Biol. Chem.* **267**, 20416–20421.

Shirabe, K., Yubisui, T. & Takeshita, M. (1989). *Biochim. Biophys. Acta*, **1008**, 189–192.

Strittmatter, P. (1965). *J. Biol. Chem.* **240**, 4481–4487.

Strittmatter, R., Kittler, J. M., Coghill, J. E. & Ozols, J. (1992). *J. Biol. Chem.* **267**, 2519–2523.

Takano, T., Bando, S., Horii, C., Higashiyama, M., Ogawa, K., Sato, M., Katsuya, Y., Danno, M., Yubisui, T., Shirabe, K. & Takeshita, M. (1994). *Flavin and Flavoproteins 1993*, edited by K. Yagi, pp. 409–412. Berlin/New York: Walter de Gruyter & Co.

Takano, T., Ogawa, K., Sato, M., Bando, S. & Yubisui, T. (1987). *J. Mol. Biol.* **195**, 749–750.

Wierenga, R. K., DcMaeyer, M. C. H. & Hol, W. G. J. (1985). *Biochemistry*, **24**, 1346–1357.

Wu, Y. S., Huang, C. H., Wan, Y., Huang, Q. J. & Zhu, Z. (1998). *J. Hematother.* **102**, 575–577.

Xia, Z.-X. & Mathews, F. S. (1990). *J. Mol. Biol.* **212**, 837–863.

Yubisui, T., Miyata, T., Iwanaga, S., Tamura, M., Yoshida, S., Takeshita, M. & Nakajima, H. (1984). *J. Biochem.* **96**, 579–582.